UV-Induced Oxo → Hydroxy Unimolecular Proton-Transfer Reactions in Hypoxanthine

Anna Gerega, Leszek Lapinski, Maciej J. Nowak,* and Hanna Rostkowska

Institute of Physics, Polish Academy of Sciences, Al. Lotnikow 32/46, 02-668 Warsaw, Poland

Received: June 7, 2006; In Final Form: July 7, 2006

Monomers of hypoxanthine isolated in low-temperature Ar matrixes were studied using Fourier transform infrared spectroscopy. Two most stable tautomeric forms of hypoxanthine: oxo-N(9)−H and oxo-N(7)−H as well as a very small amount of the minor hydroxy-N(9)−H tautomer were observed in Ar matrixes directly after their deposition. UV irradiation of the matrixes induced conversion of the oxo-N(9)−H and oxo-N(7)−H tautomers of the compound into the hydroxy-N(9)−H and hydroxy-N(7)−H forms, respectively. Upon exposure of the matrixes to the UV ($\lambda > 270$ nm) light, the oxo-N(9)−H → hydroxy-N(9)−H phototautomeric reaction dominated strongly over the oxo-N(7)−H → hydroxy-N(7)−H phototransformation. The latter phototautomeric reaction occurred effectively when matrix-isolated hypoxanthine was irradiated with shorter-wavelength ($\lambda > 230$ nm) UV light. Thanks to this wavelength dependency, it was possible to clearly distinguish the oxo → hydroxy photoreaction within the N(9)−H tautomers from the analogous phototautomeric process within the N(7)−H tautomers. All of the observed isomers of hypoxanthine (substrates and products of the photoreactions) were identified by comparison of their IR spectra with the spectra calculated at the DFT-(B3LYP)/6-31++G(d,p) level of theory.

Introduction

tRNAs contain a number of unusual bases that are not normally found in DNA or other RNAs. These modified bases influence the tRNA−mRNA base pairing and play a role in degeneracy of the genetic code.[1−3] Some tRNAs recognize only one codon, but there are some others which can recognize several different codons in mRNA. Crick suggested that the base at the 5′ end of the anticodon in tRNA does not have as strict base-pairing requirements as the other two base pairs, allowing formation of wobble pairs with several bases at the 3′ end of the codon.[4,5] This is especially true when the nucleoside at the 5′ end of the anticodon is inosine, a nucleoside that has hypoxanthine as a base. In bacteria, inosine can form wobble pairs with uridine, cytidine, and adenosine, and in eukaryotes only with uridine and cytidine. Inosine has been detected first in tRNA[6] and only after more than two decades in other RNAs, such as double-stranded RNAs, mRNAs, and virial RNAs.[7]

Inosine is formed from adenosine during enzymatic modification in tRNA. The adenine-to-inosine RNA editing is a post-transcriptional (or co-transcriptional), site-selective enzymatic process common in eukaryotes and eubacteria. Inosine monophosphate (IMP) is an intermediate in biosynthesis and in catabolism of purine nucleotides. By de novo biosynthesis of purine nucleotides, IMP is the first product with a purine structural frame built.[8] The nucleotide with hypoxanthine base is a crucial intermediate in salvage pathways of biosynthesis of purine nucleotides and in metabolic destruction of these species.[9]

Due to the role played by inosine in living organisms, the hypoxanthine base itself also receives significant interest. Neutron diffraction studies pointed out that in the crystalline phase the molecules of hypoxanthine exist predominantly in oxo-N(9)−H tautomeric form with an approximately planar purine ring; however, a minor contribution from other tautomers of hypoxanthine could not be excluded with certainty.[10]

* To whom correspondence should be addressed. E-mail: mjnow@ifpan.edu.pl.

Tautomerism involving change of position of a proton within the five-membered ring has been proposed on the basis of spectroscopic studies of neutral hypoxanthine in solutions.[11−13] These studies suggest that the relative population of the predominant tautomeric species is strongly dependent on the solvent dielectric constant. The theoretical Monte Carlo calculations of the thermodynamic properties of water solutions of hypoxanthine[14] showed that the oxo-N(9)−H tautomer would only be slightly favored as compared with the oxo-N(7)−H form. According to these results, for neutral hypoxanthine in aqueous solutions, the populations of both tautomers should be similar.

For isolated molecules of hypoxanthine, the theoretical calculations of relative energies of tautomers were carried out at the MP2 level (by Ramaekers et al.[15] and by Hernandez et al.[16]) and at the DFT level (by Shukla and Leszczynski[17] and by Hernandez et al.[16]). According to the calculations performed at the MP2/6-31+G(d,p) level,[16] the oxo-N(7)−H tautomer should be the most stable, whereas the oxo-N(9)−H form is predicted to be higher in energy only by 3.8 kJ mol^{-1}. For the hydroxy-N(9)−H and the hydroxy-N(7)−H tautomers of hypoxanthine, the calculated energies are significantly higher (by 11.7 and 21.3 kJ mol^{-1}, respectively) than the energy of the most stable oxo-N(7)−H form. Similar values of the relative energies of hypoxanthine tautomers were obtained at the MP2/6-31++G(d,p),[15] DFT(B3LYP)/6-311++G(d,p),[17] and DFT-(B3LYP)/6-31+G(d,p)[16] levels of theory. The experimental matrix-isolation studies performed hitherto[15,18,19] suggested that monomers of hypoxanthine isolated in low-temperature matrixes adopt predominantly the oxo-N(7)−H and oxo-N(9)−H tautomeric forms. Spectral signatures of a small amount (less than 5%) of hydroxy form[15,19] were also reported. Hence, although these experimental studies suffered from technical imperfections and provided no reliable method for distinguishing between the IR bands due to different tautomers, they seemed to confirm the theoretical predictions.

10.1021/jp063533o CCC: $33.50
Published on Web 08/09/2006

Photoinduced, intramolecular proton-transfer reaction converting the oxo tautomer of 4-(*3H*)-pyrimidinone into the hydroxy form was previously observed for the compound isolated in low-temperature Ar, Xe, and N_2 matrixes.[20−22] Because of the structural similarity of 4-(*3H*)-pyrimidinone and hypoxanthine, one could expect occurrence of the oxo → hydroxy phototautomeric reaction also for the latter species. Very recently, similar photoreactions were also observed for allopurinol and 9-methylhypoxanthine in argon matrixes.[23]

In the present work, unimolecular phototautomerization processes were studied for matrix-isolated hypoxanthine. The IR spectra of the substrates and products of these photoreactions were interpreted by comparison with the results of the DFT-(B3LYP)/6-31++G(d,p) calculations.

Experimental Section

The sample of hypoxanthine used in the present study was a commercial product supplied by Aldrich. The solid compound was electrically heated to ca. 500 K in a glass miniature oven placed in the vacuum chamber of a continuous-flow helium cryostat. The vapors of the compound were deposited, together with a large excess of inert gas (argon), on a CsI window cooled to 10 K. The argon matrix gas of spectral purity 6.0 was supplied by Linde AG. The IR spectra were recorded with 0.5 cm^{-1} resolution using the Thermo Nicolet Nexus 670 FTIR spectrometer equipped with a KBr beam splitter and a DTGS detector. Intensities of the IR absorption bands were measured by numerical integration. Matrixes were irradiated with light from HBO200 high-pressure mercury lamp. This lamp was fitted with a water filter and a suitable cutoff filter transmitting light with $\lambda > 270$ nm or with $\lambda > 230$ nm.

Computational Section

The geometries of isomers of hypoxanthine considered in this work were optimized using the hybrid Hartree−Fock and density functional theory method DFT(B3LYP) with the Becke's three-parameter exchange functional[24] and gradient-corrected functional of Lee, Yang, and Parr.[25] At the optimized geometries, the DFT(B3LYP) harmonic vibrational frequencies and IR intensities were calculated. All quantum-mechanical calculations were performed with the *Gaussian 98* program[26] using the 6-31++G(d,p) basis set. To correct for the systematic shortcomings of the applied methodology (mainly for anharmonicity), the predicted vibrational wavenumbers were scaled down by a single factor of 0.98. The theoretical normal modes, calculated for the tautomers of hypoxanthine, were analyzed by carrying out the potential energy distribution (PED) calculations. Transformations of the force constants with respect to the Cartesian coordinates to the force constants with respect to the molecule-fixed internal coordinates allowed the normal-coordinate analysis to be performed as described by Schachtschneider.[27] The internal coordinates used in this analysis were defined following the recommendations of Pulay et al.[28] These coordinates are listed in Tables S1 and S2 (Supporting Information). Potential energy distribution (PED) matrices[29] have been calculated (for the oxo-N(9)−H, oxo-N(7)−H, hydroxy-N(9)−H, and hydroxy-N(7)−H tautomers), and the elements of these matrices greater than 10% are given in Tables S3, S4, S5, and S6 (Supporting Information).

Results

The infrared spectrum of hypoxanthine monomers isolated in an argon matrix, recorded in the present study, is not quite identical to the spectra reported previously.[15,18,19] The most striking difference concerns the region 3520−3400 cm^{-1}, where the bands due to N−H stretching vibrations are expected. The band at 3464 cm^{-1} was reported in all of the previous papers as the strongest absorption in this range. However, in the IR spectra recorded within the present work, no absorption appears at this frequency (see Figure 1). This shows that a significant amount of species other than hypoxanthine monomers were present in matrixes reported by other authors.[15,18,19] The presence of some impurities was also indicated by the appearance of 15 other IR bands reported by other authors but missing in the spectra recorded within the current work.

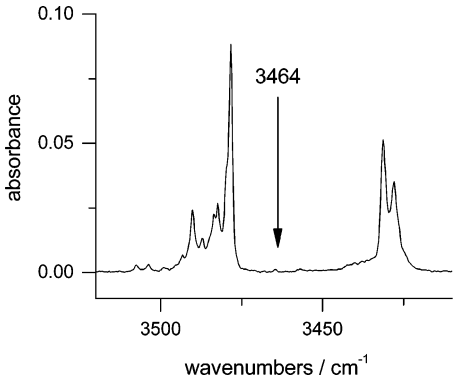

Figure 1. The high-frequency region of the IR spectrum of hypoxanthine isolated in an Ar matrix. Arrow indicates the position of the absorption band reported by other authors but absent in the spectra collected within the present work.

CHART 1: Tautomeric Forms of Hypoxanthine

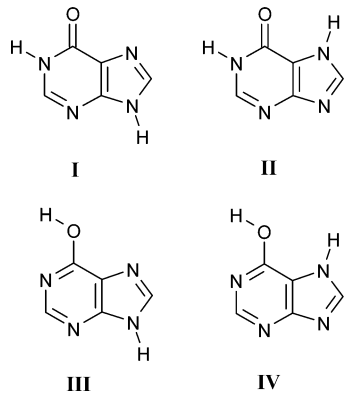

According to the theoretical calculations of relative energies of tautomeric forms of hypoxanthine, both oxo-N(9)−H form (**I**) and oxo-N(7)−H form (**II**) (see Chart 1) should be populated in the gas phase in comparable quantities, with somewhat higher population of the latter tautomer. Such a predominance of the oxo-N(7)−H tautomer in the gas phase was previously observed by means of UV photoelectron spectroscopy.[30] As a consequence, these oxo forms (**II** and **I**) should be also trapped into a low-temperature matrix. The comparison of the experimental spectrum of hypoxanthine monomers with the theoretical spectra calculated for the oxo-N(9)−H form (**I**) and for the oxo-N(7)−H form (**II**) is presented in Figure 2. This comparison strongly suggests that both tautomeric forms are present in the low-temperature matrix.

The main objective of the present work was separation of the experimental spectra of the oxo-N(9)−H and oxo-N(7)−H tautomers and generation of the hydroxy-N(9)−H form (**III**) and the hydroxy-N(7)−H form (**IV**). We attempted to meet this goal by using UV-induced oxo → hydroxy phototautomeric reaction. Phototransformation of the oxo form of 9-methyl-

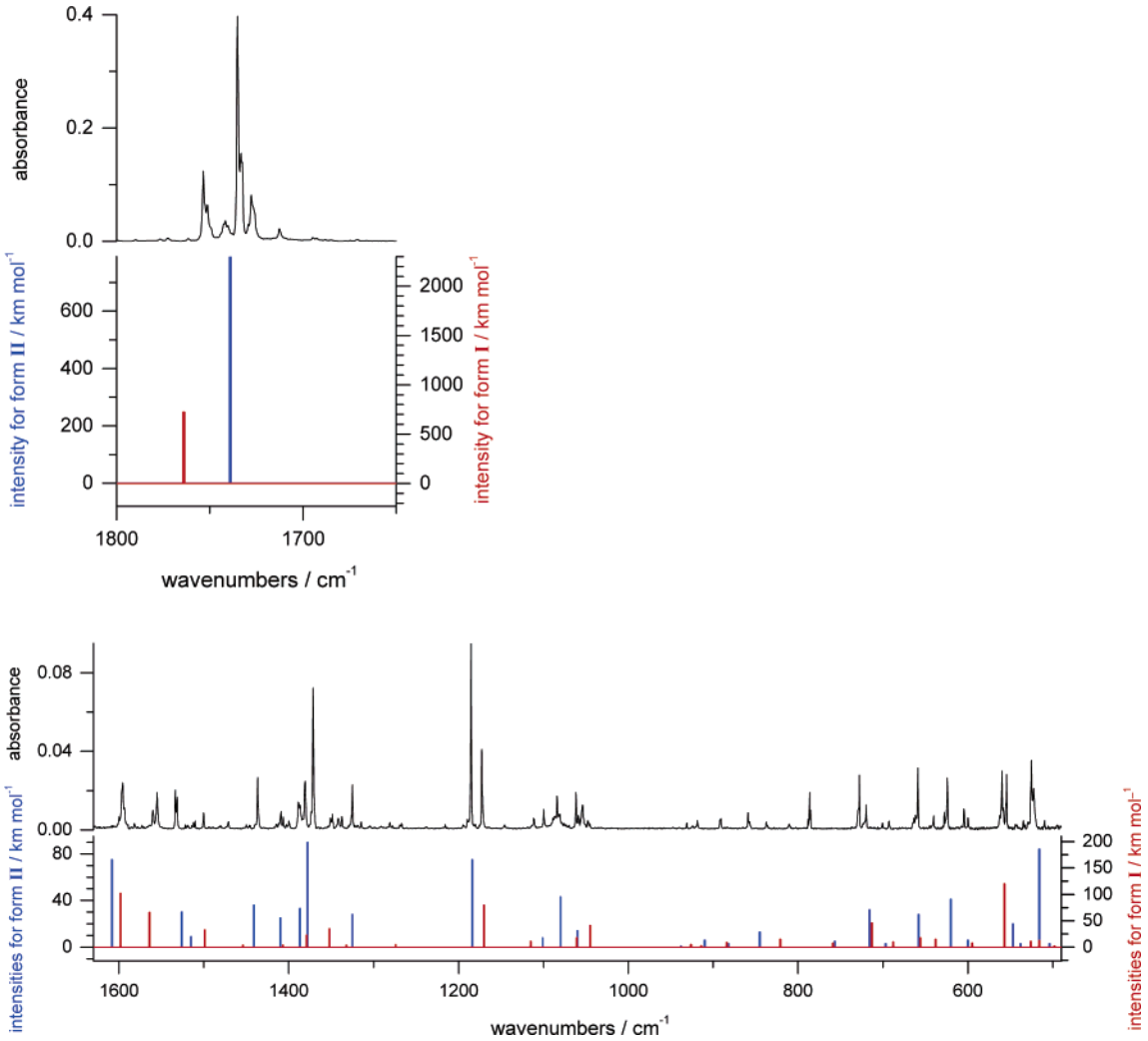

Figure 2. The IR spectrum of hypoxanthine isolated in an Ar matrix (10 K) compared with the results of theoretical simulations of the spectra: (blue sticks) for the oxo-N(7)−H tautomer (**II**) and (red sticks) for the oxo-N(9)−H tautomer (**I**). The calculated, at DFT(B3LYP)/6-31++G(d,p) level, wavenumbers were scaled by the single factor of 0.98.

hypoxanthine into the hydroxy tautomer, observed[23] very recently for the compound isolated in an Ar matrix, allowed for optimistic expectations also for hypoxanthine itself.

Upon UV (λ > 270 nm) irradiation of matrix-isolated hypoxanthine, one set of IR bands substantially decreased in intensity, whereas the bands belonging to another set were almost unchanged (Figure 3). For example, the band due to the stretching vibration of the C═O group (νC═O) observed at 1753 cm^{-1} decreased strongly, but a band due to the same type of vibration, found at 1735 cm^{-1} in the spectrum of the other oxo tautomer, did not. Comparison with the spectra theoretically predicted at the DFT(B3LYP)/6-31++G(d,p) level (Figures 2 and 3) suggests that these two bands should be assigned to the oxo tautomers **I** and **II**, respectively. The lower frequency of the νC═O vibration in molecules adopting the oxo-N(7)−H form **II** reflects the effect of the interaction between the N(7)−H proton and the lone-electron pair from oxygen atom of the C═O group. This interaction is much weaker than a typical hydrogen bonding. Also, the analysis of other regions of IR spectra (presented in Figure 3) recorded before and after UV (λ > 270 nm) irradiation confirms the assignment of structure **I** to the form being the substrate significantly consumed in the photoreaction induced by exposure to UV (λ > 270 nm) light.

Decrease of the population of form **I** was accompanied by generation of a photoproduct. If the photoreaction consuming tautomer **I** is a phototautomeric reaction presented in Scheme 1, then the photoproduct generated in this photoprocess should have the hydroxy-N(9)−H structure **III**. It is noteworthy that the bands due to the product of the phototransformation of form **I** grow at the positions of very weak absorptions present already (see Figure 4) in the spectrum collected before exposure of the matrix to UV (λ > 270 nm) light. One of these bands was observed at 3566/3561 cm^{-1} that is at a typical frequency of the O−H stretching vibrations (νO−H). Analogous (νO−H) bands in the spectra of the hydroxy forms of related compounds, allopurinol and 9-methylhypoxanthine were found at very similar frequencies: 3564 and 3557 cm^{-1}, respectively.[23] These experimental facts strongly suggest that the photoproduct is the hydroxy-N(9)−H form **III** and that a very small amount of this tautomer was present in the Ar matrix before any irradiation.

On the basis of the effects induced by UV (λ > 270 nm) irradiation of matrix-isolated hypoxanthine, it was possible to assign the bands found in the IR spectrum of the compound to the separated spectra of the oxo-N(9)−H (**I**), oxo-N(7)−H (**II**), and hydroxy-N(9)−H (**III**) tautomeric forms. For most of the observed IR bands, this assignment could be done in the unequivocal manner; somewhat less certain assignments concern cases of significant overlap of bands due to two or three tautomers. The spectrum of the bands substantially decreasing

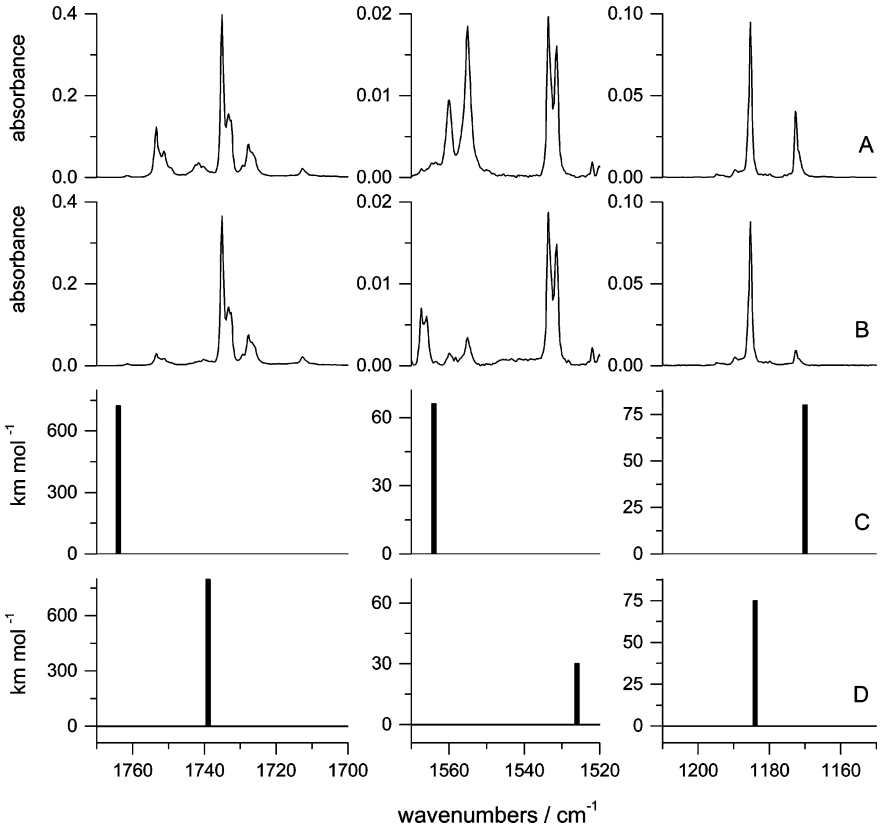

Figure 3. Fragments of the IR spectrum of hypoxanthine isolated in an Ar matrix: (A) after deposition of the matrix, (B) after 4 h of UV (λ > 270 nm) irradiation; compared with corresponding fragments of the spectrum calculated at the DFT(B3LYP)/6-31++G(d,p) level for (C) the oxo-N(9)−H tautomer and (D) the oxo-N(7)−H tautomer of the compound. The calculated wavenumbers were scaled by a factor of 0.98.

SCHEME 1: Unimolecular Oxo → Hydroxy Photoreactions in Hypoxanthine

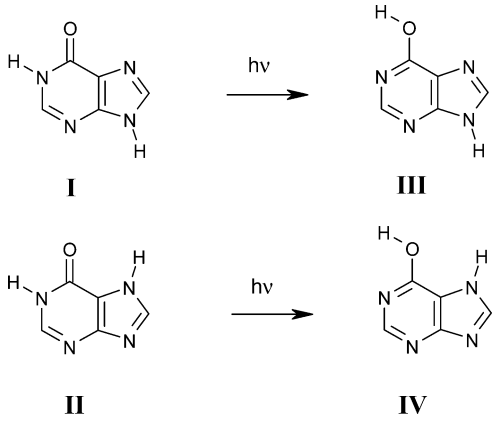

during UV (λ > 270 nm) irradiation (decreasing in the same manner as the νC═O band at 1753 cm^{-1}) is graphically presented in Figure 5C. The spectrum of the bands decreasing only slightly during UV (λ > 270 nm) irradiation (behaving in the same manner as the νC═O band at 1735 cm^{-1}) is shown in Figure 5A. These two experimental spectra are well-reproduced by the results of the theoretical predictions of the spectra of form **I** (Figure 5D) and of form **II** (Figure 5B), respectively. The very good agreement between experimental and theoretical spectra presented in Figure 5 leaves no doubt about the correctness of identification of forms **I** and **II**.

The list of IR bands observed in the initial spectrum of hypoxanthine isolated in a low-temperature Ar matrix is given in Table 1. These bands are assigned to a particular tautomeric form **I**, **II**, or **III** and interpreted by comparison with the spectra calculated at the DFT(B3LYP)/6-31++G(d,p) level. The theoretical spectra of tautomers of hypoxanthine are presented in the Supporting Information in Tables S3−S6. These tables also provide detailed PED analysis of the calculated normal modes.

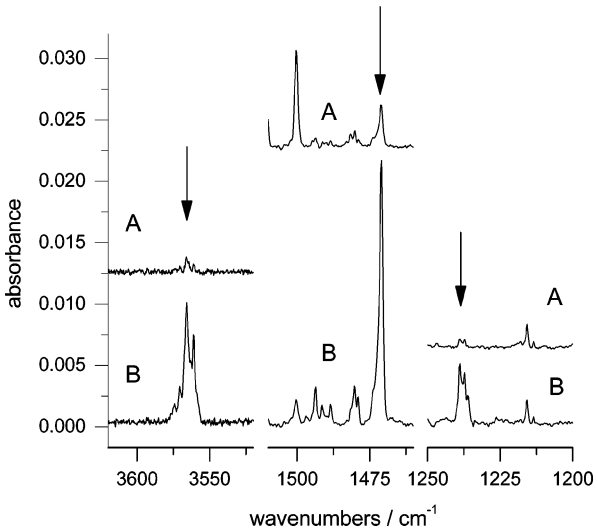

Figure 4. Fragments of the IR spectrum of hypoxanthine isolated in an Ar matrix: (A) after deposition of the matrix, (B) after 4 h of UV (λ > 270 nm) irradiation. Arrows indicate the positions of the weak absorption bands present in the initial spectrum and growing upon UV (λ > 270 nm) irradiation. These bands are the spectral signatures of the hydroxy-N(9)−H tautomer.

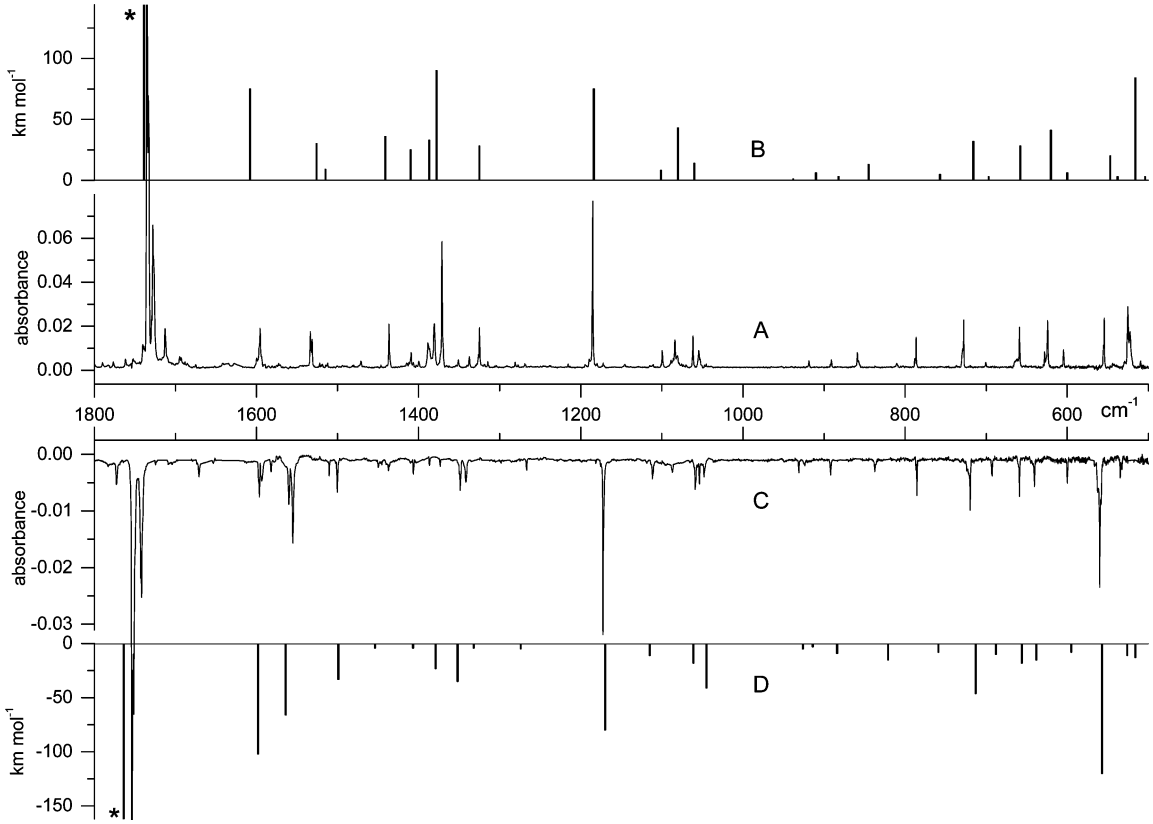

Figure 5. Comparison of the spectra of two substrates of the observed photoreactions: (C) spectrum of the bands significantly decreasing upon UV (λ > 270 nm) irradiation (showing the same behavior as the band at 1753 cm^{-1} presented in Figure 2), (A) spectrum of the bands only slightly decreasing upon UV (λ > 270 nm) irradiation (showing the same behavior as the band at 1735 cm^{-1} presented in Figure 2), with the spectra calculated at the DFT(B3LYP)/6-31++G(d,p) level for (B) the oxo-N(7)−H tautomer and (D) the oxo-N(9)−H tautomer of hypoxanthine. The calculated wavenumbers were scaled by a factor of 0.98.

An attempt was made to estimate the ratio of tautomers of hypoxanthine trapped in the low-temperature Ar matrix. The ratio of populations of the oxo-N(9)−H and the oxo-N(7)−H forms was estimated using eq 1

$$k_1 = \frac{[\mathbf{I}]}{[\mathbf{II}]} = \frac{\sum I_{\mathbf{I}}}{\sum A_{\mathbf{I}}^{\mathrm{th}}} \cdot \frac{\sum A_{\mathbf{II}}^{\mathrm{th}}}{\sum I_{\mathbf{II}}} = 0.51 \qquad (1)$$

where

$\sum I_{\mathbf{I}}$ and $\sum I_{\mathbf{II}}$ are the sums of intensities of experimental bands that could be safely assigned to the oxo-N(9)−H and the oxo-N(7)−H forms, respectively;

$\sum A_{\mathbf{I}}^{\mathrm{th}}$ and $\sum A_{\mathbf{II}}^{\mathrm{th}}$ are the sums of the absolute intensities of corresponding bands in the spectra theoretically calculated for the oxo-N(9)−H and the oxo-N(7)−H tautomers, respectively.

The strongly overlapping bands due to N−H stretching vibrations were not taken into account in this assessment. Assuming that the observed ratio of tautomers (k_1 = 0.51) corresponds to the frozen gas-phase equilibrium at the temperature of evaporation of the compound (T = 500 K), the free energy difference between the two oxo forms was estimated as ΔE = 2.8 kJ mol^{-1} in favor of form **II**. This value matches nicely (within ±1.5 kJ mol^{-1}) the theoretical predictions.

In the case of oxo−hydroxy tautomeric equilibrium, the situation is more complicated. Because of the small initial population of the hydroxy-N(9)−H form **III**, infrared bands due to this tautomer are very weak. Hence, the assessment of k_2 = [**III**]/[**I**] using the same method as in the case of k_1 would suffer from substantial uncertainty. Nevertheless, such an effort was undertaken, and the resulting ratio of the hydroxy-N(9)−H form to the oxo-N(9)−H form was 0.1 ± 0.03.

Such values of k_1 and k_2 mean that after deposition of the matrix tautomers **II**, **I**, and **III** are present in the ratio of 1:0.51:0.05.

To assess the relative population of tautomeric form **III**, another method has also been applied. This approach was based on the changes of populations of the oxo-N(9)−H form **I** and hydroxy-N(9)−H form **III** during the transformation **I** → **III**, induced by UV (λ > 270 nm) light. Consumption of form **I** and generation of form **III** can be described by eq 2

$$[\mathbf{I}]_{\mathrm{i}} - [\mathbf{I}]_{\mathrm{f}} = [\mathbf{III}]_{\mathrm{f}} - [\mathbf{III}]_{\mathrm{i}} \qquad (2)$$

where

$[\mathbf{I}]_{\mathrm{i}}$ and $[\mathbf{III}]_{\mathrm{i}}$ are populations of forms **I** and **III** before UV irradiations;

$[\mathbf{I}]_{\mathrm{f}}$ and $[\mathbf{III}]_{\mathrm{f}}$ are populations of forms **I** and **III** after UV irradiations.

Equation 2 is strictly valid as far as the **I** → **III** conversion is quantitative.

On the basis of the experimental spectra, collected before and after UV (λ > 270 nm) irradiation, the following values were obtained: $[\mathbf{III}]_{\mathrm{f}}/[\mathbf{III}]_{\mathrm{i}}$ = 8.3 and $[\mathbf{I}]_{\mathrm{f}}/[\mathbf{I}]_{\mathrm{i}}$ = 0.24.

By combination of these relations with eq 2, the ratio of populations of forms **III** and **I** was assessed

$$k_2' = \frac{[\mathbf{III}]_{\mathrm{i}}}{[\mathbf{I}]_{\mathrm{i}}} = \frac{1 - \dfrac{[\mathbf{I}]_{\mathrm{f}}}{[\mathbf{I}]_{\mathrm{i}}}}{\dfrac{[\mathbf{III}]_{\mathrm{f}}}{[\mathbf{III}]_{\mathrm{i}}} - 1} = 0.1 \qquad (3)$$

TABLE 1: Spectral Positions and Relative Intensities of the Absorption Bands Found in the IR Spectrum of Hypoxanthine Isolated in an Ar Matrix (10 K)[a]

wavenumbers cm^{-1}	relative intensity	form	normal mode number[b]	description of the mode[b]	wavenumbers cm^{-1}	relative intensity	form	normal mode number[b]	description of the mode[b]
3566, 3561	0.5	**III**[c]			**1239**, 1237	0.2	**III**[c]		
3490, 3484, **3482**	18.3	**I**	Q1	ν N9H	1190, **1185**	12.7	**II**	Q15	β CH, β ring, ν ring
3478	18.5	**II**	Q1	ν N7H	**1173**, 1172	5.7	**I**	Q15	β CH, β ring
3431	15.9	**II**	Q2	ν N1H	1112, 1111	1.3	**II**	Q16	ν ring, β N1H
3428	11.4	**I**+**II**	Q2	ν N1H	1101, **1100**	1.7	**I**	Q16	ν ring, β N1H
1772	1.5	**I**			1087	0.4	**I**		
1753, 1751, 1742	50.9	**I**	Q5	ν C=O	1089, **1084**, 1081	7.0	**II**	Q17	ν ring, β N7H, β CH
1735, 1733, 1727	106.3	**II**	Q5	ν C=O	1074	0.1	**III**[c]		
1712	5.9	**II**			**1062**, 1055	5.5	**II**	Q18	ν ring, β ring, β C=O
1642, 1635	0.4	**III**			**1059**, 1058	1.1	**I**	Q17	ν ring, β N9H
1600, **1596**	9.7[d]	**II**	Q6	ν ring	1048	0.5	**I**	Q18	ν ring, β C=O
1597, 1593	overlap[d]	**I**	Q6	ν ring	931	0.3	**I**	Q19	β ring
1582	0.4	**I**			925	0.1	**III**[c]		
1560, **1555**	7.1	**I**	Q7	ν ring	924	0.2	**I**	Q20	γ CH
1534, 1531	4.8	**II**	Q7	ν ring	919	0.8	**II**	Q20	γ CH
1522, 1519, 1515, 1512	0.9	**II**			892	0.6	**I**	Q21	β ring
1510	0.3	**I**			891	0.5	**II**	Q21	β ring
1500	1.2	**I**	Q8	ν ring	886	0.1	**III**[c]		
1471	0.7	**III**[c]			**859**, 858	1.7	**II**	Q22	γ CH
1450	0.3	**I**	Q9	ν ring, β N1H	837	0.5	**I**	Q22	γ CH
1437	4.2	**II**	Q9	ν ring, β CH, β ring	811	0.4	**II**		
1415, 1412, **1409**	2.4	**II**	Q10	β N1H, β N7H, ν ring	788, **787**, 785	2.7[d]	**II**	Q23	τ ring
1407	0.5	**I**	Q10	β N1H, ν ring, β CH	787, 785	overlap[d]	**I**	Q23	γ C=O, τ ring
1400	0.8	**II**			729, **728**	4.1	**II**	Q24	γ C=O, γ N1H
1388, 1387, **1381**	11.9	**II**	Q11	β CH, ν ring	720	2.4	**I**	Q24	γ N1H, γ C=O
1373	0.4	**I**	Q11	β N9H, β CH, ν ring	701	0.4	**II**	Q25	ν ring
1371	9.9	**II**	Q12	ν ring, β N7H	693	0.6	**I**	Q25	ν ring
1351	0.7	**II**			659	4.4[d]	**II**	Q26	γ N1H, τ ring
1350, **1349**	1.3	**I**	Q12	ν ring, β CH	659	overlap[d]	**I**	Q26	τ ring
1342	1.6	**I**	Q13	ν ring, β CH	641	0.8	**I**	Q27	τ ring, γ N1H
1330	0.1	**III**[c]			628, **624**	4.7	**II**	Q27	τ ring, γ N1H
1326, 1325	3.3	**II**	Q13	β CH, ν ring	605	1.2	**II**	Q28	β ring, ν ring, β C=O
1319, 1318	0.2	**III**[c]			600	0.6	**I**	Q28	β ring, ν ring, β C=O
1315	0.5	**II**			563, **560**, 558	7.0	**I**	Q29	γ N9H, τ ring
1281, 1278	0.5	**II**			555, **554**	3.9	**II**	Q29	τ ring
1269	0.4	**III**[c]			535, 533	0.8	**I**	Q30	β ring, β C=O
1267	0.3	**I**	Q14	β CH, ν ring	**526**, 523	11.9	**II**	Q31	γ N7H
					510	0.7	**II**	Q32	β ring

[a] Wavenumbers of the most intense components of split bands are bold-faced. [b] The spectra calculated at the DFT(B3LYP)/6-31++G(d,p) level for tautomers **I**, **II**, and **III** are given in Supporting Information Tables S3, S4, and S5, respectively. The full PED analysis of the normal modes is also provided in these tables. In-plane vibrations: ν stretching, β bending. Out-of-plane vibrations: γ wagging, τ torsional. [c] For assignment of the bands due to hydroxy-N(9)−H tautomer **III,** see Table 2. [d] Summaric intensity of overlapping bands.

Because upon exposure of matrix-isolated hypoxanthine to UV ($\lambda > 270$ nm) light the oxo → hydroxy phototautomeric reaction was accompanied by a minor photodecomposition process (see the spectral signatures in the Figures 6 and 7), the value k_2' must be treated as an upper limit of the ratio of forms **III** and **I** in the Ar matrix before any irradiation. Nevertheless, as could be seen, both methods of evaluation of relative populations of form **III** gave the same values $k_2 = k_2' = 0.1$.

For the temperature $T = 500$ K, the free energy difference between forms **I** and **III** corresponding to the k_2 value is equal to (9.6 ± 1) kJ mol^{-1} in favor of oxo-N(9)−H form **I**. This value nicely fits the energy difference for tautomers **I** and **III** calculated at the MP2 level by Ramaekers et al.[18] (MP2/6-31++G**; $\Delta E = 8.25$ kJ mol^{-1}) and Hernandez et al.[16] (MP2/6-31+G(d,p); $\Delta E = 7.95$ kJ mol^{-1}).

The oxo−hydroxy equilibrium observed within N(9)−H tautomers of hypoxanthine is quite similar to that recently investigated for 9-methylhypoxanthine.[23] For the latter compound, the ratio of the oxo and hydroxy tautomers trapped in an Ar matrix was 11.7:1, whereas for hypoxanthine, the analogous ratio was approximately equal to 10:1. It could be anticipated that tautomerism, in which N(1) and O atoms are directly involved, would not be significantly influenced by the replacement of the hydrogen atom by a methyl group at the remote N(9) position. Hence, it is not surprising that the experimentally estimated difference of free energies (9.8 kJ mol^{-1} at $T = 480$ K) of the hydroxy and oxo tautomers of 9-methylhypoxanthine[23] is so similar to the corresponding value obtained for the hydroxy and oxo-N(9)−H tautomers of hypoxanthine (9.6 kJ mol^{-1} at $T = 500$ K).

Whereas irradiation of matrix-isolated hypoxanthine with UV ($\lambda > 270$ nm) light led only to slight consumption of the oxo-N(7)−H tautomer **II** and to generation of correspondingly small amount of the hydroxy-N(7)−H form **IV**, the phototautomeric **II** → **IV** transformation was considerably more pronounced when the matrixes were exposed to shorter-wavelength UV ($\lambda > 230$ nm) light. The spectra shown in Figure 6 demonstrate the dependency of relative effectiveness of **II** → **IV** and **I** → **III** phototautomeric reactions on the wavelength of UV light used for irradiation. The bigger amount of the hydroxy-N(7)−H tautomer **IV** generated upon UV ($\lambda > 230$ nm) irradiation is evidenced by much higher intensity of the band at 1566 cm^{-1} (Figure 6C), in comparison to the intensity of this band in the spectrum recorded after irradiation of the matrix with UV ($\lambda > 270$ nm) light (Figure 6B). The IR band at 1566 cm^{-1} is a very characteristic feature, which can reliably be assigned to the spectrum of the hydroxy-N(7)−H form **IV**. The experimental spectra of photoproducts generated upon UV ($\lambda > 230$ nm) irradiation and upon UV ($\lambda > 270$ nm) irradiation are compared (in Figure 7) with the spectra theoreti-

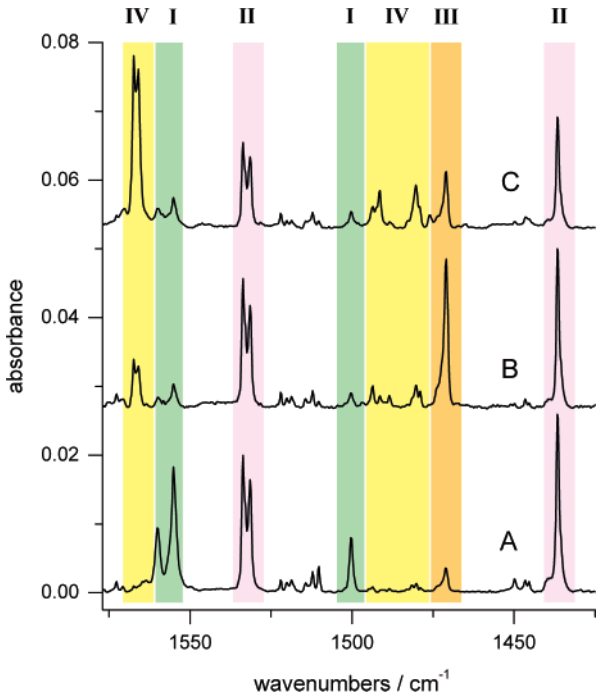

Figure 6. Fragment of the IR spectrum of hypoxanthine isolated in an Ar matrix: (A) after deposition of the matrix; (B) after 4 h of UV (λ > 270 nm) irradiation; (C) recorded in a separate experiment after 2 h of UV (λ > 230 nm) irradiation of the matrix. Infrared bands due to different tautomers of hypoxanthine are marked with different color of the background: (green) oxo-N(9)−H; (violet) oxo-N(7)−H; (orange) hydroxy-N(9)−H; (yellow) hydroxy-N(7)−H. Intensities of the bands recorded in the two experiments are normalized by the factor correcting for the slightly different amount of the compound deposited in both experiments.

cally predicted for the hydroxy tautomers **III** and **IV**. This comparison supports the conclusion that exposure of matrix-isolated hypoxanthine to UV light leads to phototautomeric reactions **I** → **III** and **II** → **IV** (Scheme 1), with the first process relatively more effective upon (λ > 270 nm) irradiation and the second process more pronounced upon (λ > 230 nm) irradiation. The bands which could be reliably assigned to the spectra of hydroxy tautomers **III** and **IV** are listed in Table 2. These bands are also compared with the results of theoretical predictions and interpreted in terms of DFT-calculated normal modes.

Alongside the IR bands, which should be assigned to photoproducts **III** and **IV**, several other bands appear in the spectra recorded after UV irradiation. One of these IR absorptions (a broad and structured feature at 2144 cm^{-1}) indicates photogeneration of the open-ring conjugated ketene. Analogous bands (due to "antisymmetric" stretching vibrations of the −C═C═O group) were observed at 2153, 2151, and 2139 cm^{-1} in the IR spectra of UV-irradiated allopurinol, 9-methylhypoxanthine, and 4-(*3H*)-pyrimidinone, respectively.[21−23] Other bands (e.g., those shown in Figure 7) indicating occurrence of unidentified phototransformations accompanying the **II** → **IV** and **I** → **III** phototautomerism are listed in Table S7 (Supporting Information). These bands already appear upon UV (λ > 270 nm) irradiation of matrix-isolated hypoxanthine. The yield of unidentified photoproducts, other than the hydroxy tautomers **III** and **IV**, was higher when the shorter-wavelength UV (λ > 230 nm) light was used. Photogeneration of these species was even more pronounced when matrixes were exposed to unfiltered light of the high-pressure mercury lamp (λ > 200 nm).

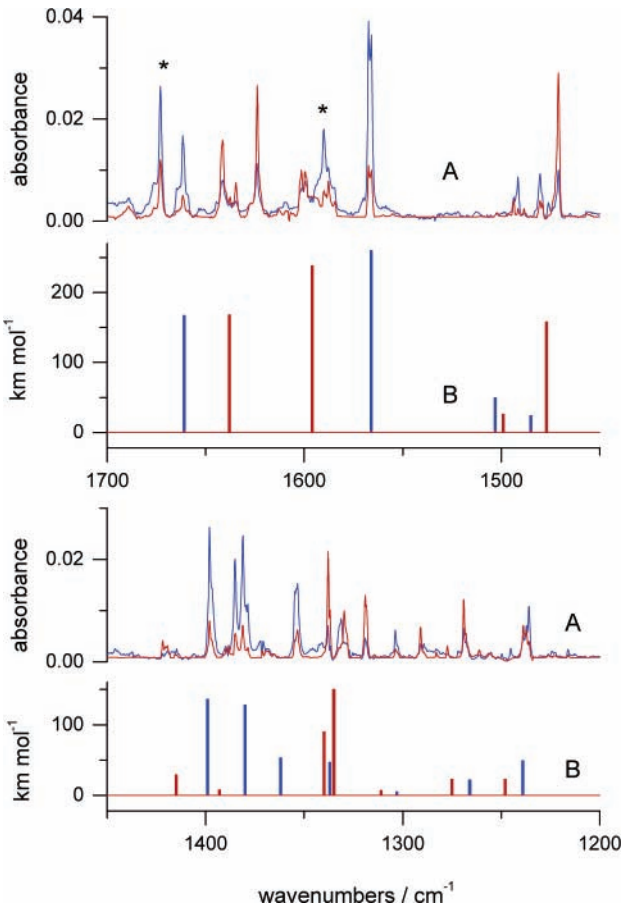

Figure 7. Panel (A). Fragments of the experimental spectra of photoproducts: (red line) generated upon UV (λ > 270 nm) irradiation, (blue line) generated upon UV (λ > 230 nm) irradiation. The spectra of the oxo-N(9)−H (**I**) and oxo-N(7)−H (**II**) tautomers were removed by electronic subtraction from the spectra recorded after UV irradiation. Panel (B). The corresponding fragments of the spectra calculated at the DFT(B3LYP)/6-31++G(d,p) level for the following: (red) the hydroxy-N(9)−H tautomer (**III**) and (blue) the hydroxy-N(7)−H tautomer (**IV**) of hypoxanthine. The calculated wavenumbers were scaled by a factor of 0.98. Asterisks indicate the bands due to unidentified photoproducts other than the hydroxy tautomers **III** and **IV**.

Concluding Discussion

The oxo-N(7)−H tautomeric form **II** of hypoxanthine was observed as a dominating isomer of the compound isolated in low-temperature Ar matrixes. The second, significantly populated form was the oxo-N(9)−H tautomer **I**, in which the hydrogen atom is attached to another nitrogen atom within the imidazole ring. The oxo-N(7)−H tautomer **II** is stabilized by the interaction of the N(7)−H hydrogen atom with the lone-electron pair of C(6)═O oxygen, whereas the interaction of the N(9)−H hydrogen atom with the lone-electron pair of N(3) nitrogen stabilizes the oxo-N(9)−H form **I** (Chart 2). Apparently, the stabilizing interaction is stronger in the first case. This is due to a more favorable geometry of the quasi-ring closed by an interaction between N(7)−H and O═C(6). In this case, the distance between these groups, which form a five-membered quasi-ring, is shorter than the distance between the hydrogen atom of the N(9)−H group and the lone electron pair of N(3) nitrogen atom in tautomer **I**. Moreover, in the structure of tautomer **II**, one of the lone electron pairs of the oxygen atom is directed toward the N(7)−H group. Such a favorable angular

TABLE 2: Spectral Positions of the Absorption Bands Attributed to the Hydroxy Tautomers of Hypoxanthine, Isolated in an Ar Matrix, Found in the IR Spectrum Obtained after UV Irradiations[a]

wavenumbers cm^{-1}	relative intensity	mode number[b]	description of the mode[b]
		Form **III** Hydroxy-N(9)−H	
3566, 3561	7.3	Q1	ν OH
3496	4.4	Q2	ν N9H
1642, 1635	3.9	Q5	ν ring
1624	4.8	Q6	ν ring
1471	4.8	Q8	ν ring, β CH
1421	0.8	Q9	ν ring
1338	2.7	Q11/Q12	ν ring, β CH/ν C−O, ν ring
1330	1.6	Q11/Q12	ν ring, β CH/ν C−O, ν ring
1319, 1318	2.0	Q11/Q12	ν ring, β CH/ν C−O, ν ring
1291	0.7	Q13	ν ring, β CH
1269	1.5	Q14	β OH, ν ring
1239, 1237	1.2	Q15	β CH, ν ring
1083, 1074	4.6	Q17	ν ring, β OH
925	0.4	Q20	β ring, ν ring
886	0.4	Q21	β ring
570	1.2	Q28	τ ring, γ N9H
523, 521	4.0	Q29	τ OH
		Form **IV** Hydroxy-N(7)−H	
3568, 3563	12.9	Q1	ν OH
3490	7.8	Q2	ν N7H
1662	7.2	Q5	ν ring
1566	14.4	Q6	ν ring
1492	2.1	Q7	ν ring, β CH
1480	1.7	Q8	β CH, ν ring
1398	7.6	Q9	β N7H, ν ring
1385, **1381**	10.4	Q10	ν ring
1354	5.6	Q11	ν ring
1332	2.6	Q12	β CH, ν ring
1304	0.9	Q13	ν ring, β OH
1236	2.1	Q15	β CH, β OH, ν ring
1054	7.3	Q18	ν C−O, β ring, β N7H
956, 951	1.1	Q19	γ CH
878, **875**	1.2	Q21/Q22	β ring/γ CH
490	8.2	Q31	τ OH

[a] Wavenumbers of the most intense components of split bands are bold-faced. [b] The spectra calculated at the DFT(B3LYP)/6-31++G(d,p) level for tautomers **III** and **IV** are given in Supporting Information Tables S5 and S6, respectively. The full PED analysis of the normal modes is also provided in these tables. In-plane vibrations: ν stretching, β bending. Out-of-plane vibrations: γ wagging, τ torsional.

factor does not appear in the case of interaction between N(9)−H and N(3) in the molecule of the oxo-N(9)−H-tautomer **I**.

In a molecule of purine itself (Chart 2), the only possible intramolecular interaction between a N−H hydrogen atom and a lone electron pair of some other heteroatom is that between N(9)−H and N(3). As a consequence, only the N(9)−H tautomer, stabilized by this interaction, is populated in the gas phase and in low-temperature Ne, Ar, and N_2 matrixes.[31−33] On the other hand, a very strong domination of the thione-N(7)−H tautomer was observed for 6-thiopurine[34] (Chart 2), a thione analogue of hypoxanthine considered in the present work. No traces of the thione-N(9)−H tautomer were found for 6-thiopurine isolated in low-temperature matrixes. This can be explained by the ability of the more spacious lone electron pairs of the C═S sulfur atom to interact at longer distances. Hence, for 6-thiopurine, the stabilizing effect of the attraction between N(7)−H and the lone electron pair of the S═C(6) group dominates strongly over the effect of the interaction between N(9)−H and N(3).

Juxtaposition of the results of the studies on tautomerism of purine, hypoxanthine, and 6-thiopurine evidently demonstrates

CHART 2: N(9)−H and N(7)−H Tautomeric Forms of Purine, Hypoxanthine, and 6-Thiopurine

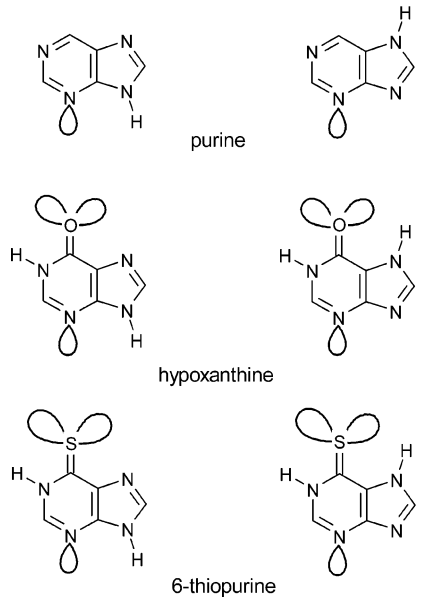

the role of intramolecular interactions between hydrogen atoms of N−H groups and the lone electron pair of other heteroatoms as an important factor governing tautomeric equilibria in purine bases.

In the current work, the IR spectra of the oxo-N(7)−H and of the oxo-N(9)−H tautomers of hypoxanthine were experimentally separated as a result of the UV-induced transformations of both forms. The previous attempts to assign the observed bands to the spectra of tautomers **I** and **II** were based on a mere comparison with the spectra theoretically predicted for the two forms.[15] In comparison to such methods, the separation of the spectra done in the present work is much more reliable.

The unimolecular proton-transfer photoreaction, observed in the present work for hypoxanthine, is most probably of the same nature as the phototautomeric processes found previously for matrix-isolated 4-(3*H*)-pyrimidinone,[20−22] 2-(1*H*)-pyridinone,[35] 9-methylhypoxanthine, and allopurinol.[23] According to the reports of Maier and Enders[36] and of Duvernay et al.,[37] an analogous oxo → hydroxy phototautomerism occurs also for the simple molecule of formamide. Recently, a similar vacuum-UV-induced intramolecular proton-transfer reaction was reported by Duvernay et al.[38] for matrix-isolated urea. The mechanism of these processes is still not well-elucidated. In this regard, the most promising ideas stem from the theoretical works of Sobolewski and co-workers.[39−41] On the basis of their CASPT2 calculations, these authors postulate a key role of excited $^1\pi\sigma^*$ states in hydrogen-atom-detachment and proton-transfer processes occurring in a variety of molecular systems.

Supporting Information Available: Chart S1 showing the atom numbering for the oxo-N(9)−H, oxo-N(7)−H, hydroxy-N(9)−H, and hydroxy-N(7)−H tautomers of hypoxanthine. Tables S1 and S2 providing definitions of the internal coordinates used in the normal-mode analysis carried out for the tautomers of hypoxanthine. Tables S3−S6 providing the results of the theoretical [DFT(B3LYP)/6-31++G(d,p)] predictions of the infrared spectra (including the PED analysis of the normal modes) of the oxo-N(9)−H, oxo-N(7)−H, hydroxy-N(9)−H, and hydroxy-N(7)−H tautomers of the compound. Table S7 listing spectral positions of IR bands due to unidentified photoproducts generated upon UV irradiation of hypoxanthine.

This material is available free of charge via the Internet at http://pubs.acs.org.

References and Notes

(1) Crick, F. H. C.; Barnett, L.; Brenner, S.; Watts-Tobin, R. J. *Nature (London)* **1961**, *192*, 1227.
(2) Nishimura, S.; Jones, D. S.; Khorana, H. G. *J. Mol. Biol.* **1965**, *13*, 302.
(3) Jukes, T. H. *Adv. Enzymol.* **1978**, *47*, 375.
(4) Crick, F. H. C. *J. Mol. Biol.* **1966**, *19*, 548.
(5) Mitra, S. K.; Ninio, J. *FEBS Symp.* **1978**, *51*, 437.
(6) Holley, R. W.; Everett, G. A.; Madison, J. T.; Zamir, A. *J. Biol. Chem.* **1965**, *240*, 2122.
(7) Grosjean, H.; Auxilien, S.; Constantinesco, F.; Simon, C.; Corda, Y.; Becker, H. F.; Foiret, D.; Morin, A.; Jin, Y. X.; Fournier, M.; Fourrey, J. L. *Biochimie* **1996**, *78*, 488.
(8) Smith, J. L. *Curr. Opin. Struct. Biol.* **1995**, *5*, 752.
(9) Stryer, L. *Biochemistry*, 4th ed.; W. H. Freeman and Company: New York, 1995.
(10) Schmalle, H. W.; Hänggi, G.; Dubler, E. *Acta Crystallogr.* **1988**, *C44*, 732.
(11) Chenon, M. T.; Pugmire, R. J.; Grant, D. M.; Panzica, R. P.; Townsend, L. B. *J. Am. Chem. Soc.* **1975**, *97*, 4636.
(12) Pullman, B.; Pullman, A. *Adv. Heterocycl. Chem.* **1971**, *13*, 77.
(13) Lichtenberg, D.; Bergmann, F.; Neiman, Z. *Isr. J. Chem.* **1972**, *10*, 805.
(14) San Roman-Zimbron, M. L.; Costas, M. E.; Acevedo-Chavez, R. *THEOCHEM* **2004**, *711*, 83.
(15) Ramaekers, R.; Maes, G.; Adamowicz, L.; Dkhissi, A. *J. Mol. Struct.* **2001**, *560*, 205.
(16) Hernandez, B.; Luque, F. J.; Orozco, M. *J. Org. Chem.* **1996**, *61*, 5964.
(17) Shukla, M. K.; Leszczynski, J. *THEOCHEM* **2000**, *529*, 99.
(18) Ramaekers, R.; Dkhissi, A.; Adamowicz, L.; Maes, G. *J. Phys. Chem. A* **2002**, *106*, 4502.
(19) Sheina, G. G.; Stepanian, S. G.; Radchenko, E. D.; Blagoi, Yu. *J. Mol. Struct.* **1987**, 158, 275.
(20) Nowak, M. J.; Lapinski, L.; Fulara, J. *J. Mol. Struct.* **1988**, *175*, 91.
(21) Lapinski, L.; Fulara, J.; Nowak, M. J. *Spectrochim. Acta* **1990**, *47A*, 61.
(22) Lapinski, L.; Nowak, M. J.; Les, A.; Adamowicz, L. *J. Am. Chem. Soc.* **1994**, *116*, 1461.
(23) Gerega, A.; Lapinski, L.; Reva, I.; Rostkowska, H.; Nowak, M. J. *Biophys. Chem.* **2006**, *122*, 123.
(24) Becke, A. *Phys. Rev. A* **1988**, *38*, 3098.
(25) Lee, C. T.; Yang, W. T.; Parr, R. G. *Phys. Rev. B* **1988**, *37*, 785.
(26) Frisch, M. J.; Trucks, G. W.; Schlegel, H. B.; Scuseria, G. E.; Robb, M. A.; Cheeseman, J. R.; Zakrzewski, V. G.; Montgomery, J. A., Jr.; Stratmann, R. E.; Burant, J. C.; Dapprich, S.; Millam, J. M.; Daniels, A. D.; Kudin, K. N.; Strain, M. C.; Farkas, O.; Tomasi, J.; Barone, V.; Cossi, M.; Cammi, R.; Mennucci, B.; Pomelli, C.; Adamo, C.; Clifford, S.; Ochterski, J.; Petersson, G. A.; Ayala, P. Y.; Cui, Q.; Morokuma, K.; Malick, D. K.; Rabuck, A. D.; Raghavachari, K.; Foresman, J. B.; Cioslowski, J.; Ortiz, J. V.; Baboul, A. G.; Stefanov, B. B.; Liu, G.; Liashenko, A.; Piskorz, P.; Komaromi, I.; Gomperts, R.; Martin, R. L.; Fox, D. J.; Keith, T.; Al-Laham, M. A.; Peng, C. Y.; Nanayakkara, A.; Gonzalez, C.; Challacombe, M.; Gill, P. M. W.; Johnson, B.; Chen, W.; Wong, M. W.; Andres, J. L.; Gonzalez, C.; Head-Gordon, M.; Replogle, E. S.; Pople; J. A. *Gaussian 98*, revision A.7.; Gaussian, Inc.: Pittsburgh, PA, 1998.
(27) Schachtschneider, J. H. *Vibrational Analysis of Polyatomic Molecules, Parts V and VI*, Technical Report; Shell Development Co., Emeryville, CA, 1964 and 1965.
(28) Pulay, P.; Fogarasi, G.; Pang, F.; Boggs, J. E. *J. Am. Chem. Soc.* **1979**, *101*, 2550.
(29) Keresztury, G.; Jalsovszky, G. *J. Mol. Struct.* **1971**, *10*, 304.
(30) Lin, J.; Yu, C.; Peng, S.; Akiyama, I.; Li, K.; Li Kao Lee; LeBreton, P. R. *J. Phys. Chem.* **1980**, *84*, 1006.
(31) Nowak, M. J.; Lapinski, L.; Kwiatkowski, J. S.; Leszczynski, J. *Spectrochim. Acta* **1991**, *47A*, 87.
(32) Nowak, M. J.; Rostkowska, H.; Lapinski, L.; Kwiatkowski, J. S.; Leszczynski, J. *Spectrochim. Acta* **1994**, *50A*, 1081.
(33) Nowak, M. J.; Rostkowska, H.; Lapinski, L.; Kwiatkowski, J. S.; Leszczynski, J. *J. Phys. Chem.* **1994**, *98*, 2813.
(34) Lapinski, L.; Nowak, M. J.; Kwiatkowski, J. S.; Leszczynski, J. *J. Phys. Chem. A* **1999**, *103*, 280.
(35) Nowak, M. J.; Lapinski, L.; Fulara, J.; Les, A.; Adamowicz, L. *J. Phys. Chem.* **1992**, *96*, 1562.
(36) Maier, G.; Endres, J. *Eur. J. Org. Chem.* **2000**, 1061.
(37) Duvernay, F.; Trivella, A.; Borget, F.; Coussan, S.; Aycard, J. P.; Chiavassa, T. *J. Phys. Chem. A* **2005**, *109*, 11155.
(38) Duvernay, F.; Chiavassa, T.; Borget, F.; Aycard, J. P. *J. Phys. Chem. A* **2005**, *109*, 6008.
(39) Sobolewski, A. L.; Domcke, W.; Dedonder-Lardeux, C.; Jouvet, C. *Phys. Chem. Chem. Phys.* **2002**, *4*, 1093.
(40) Sobolewski, A. L.; Domcke, W. *Chem. Phys.* **2000**, *259*, 181.
(41) Domcke, W.; Sobolewski, A. L. *Science* **2003**, *302*, 1693.